Enhanced electrochemical performance of MnO_2 nanoparticles: Graphene aerogels as conductive substrates and capacitance contributors

Huaxia Chen[a], Xingyu Lu[b], Lili Zhang[a,b], Dianpeng Sui[a,*], Chao Wang[c], Fanbao Meng[a], Wei Qi[b,*]

[a]*Department of Chemistry, College of Science, Northeastern University, Shenyang 110819, China*

[b]*Shenyang National Laboratory for Materials Science, Institute of Metal Research, Chinese Academy of Sciences, Shenyang 110016, China*

[c]*School of Medical Devices, Shenyang Pharmaceutical University, No. 103, Wenhua Road, Shenyang 110016, China.*

[*]Corresponding authors.

E-mail addresses: suidianpeng@mail.neu.edu.cn (D. Sui);

wqi@imr.ac.cn (W. Qi).

Capacitance calculation:

The specific capacitance (C_g, F g^{-1}) was calculated in the three-electrode system according to the following equations:

$$C_g = I \times \Delta t/(m \times \Delta V)$$

Where I is the constant discharge current (A), Δt is the discharge time (s), ΔV is the voltage window (V) during the discharge process, m is the mass of the active material on the working electrode (g).

In the two-electrode asymmetric supercapacitor system, the specific capacitance was calculated based on the mass loading of the active materials both in electrodes.

The specific capacity/capacitance is calculated based on the mass of MnO_2/NGA for MnO_2/NGA electrode, the mass of MnO_2 for MnO_2 electrode and the mass of NGA for NGA electrode, respectively.

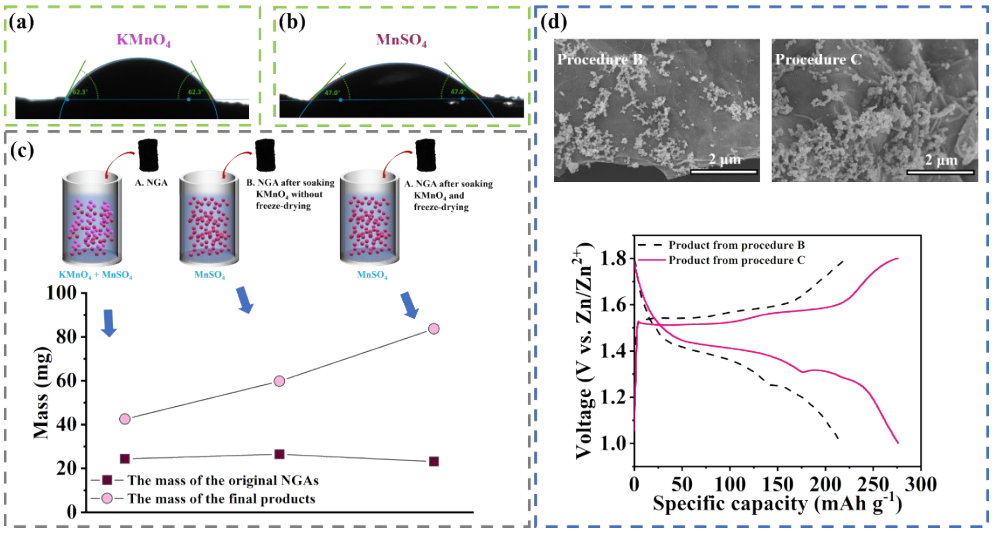

Fig. S1 (a) Contact angle of the aqueous $KMnO_4$ on the NGA. (b) Contact angle of the aqueous $MnSO_4$ on $KMnO_4$-absorbed NGA. (c) Comparisons for the weight of the original and final products from different synthetic procedures. (d) SEM images and GCD curves at 0.1 A g^{-1} of products from procedure B and C, respectively.

First of all, we observe that NGA can absorb about 8 mL $KMnO_4$ (0.1 mol L^{-1}) in the scope of 24 h. We compare the weight of the final products from different synthetic procedures as illustrated in **Fig. S1c**. Procedure A: The NGA, $KMnO_4$ and $MnSO_4$ (8 mL 0.1 mol L^{-1} $KMnO_4$ + 32 mL 0.0625 mol L^{-1} $MnSO_4$) are mixed and heated in the sealed Teflon-lined autoclave for 12 h at 120 °C. Procedure B: The NGA (after soaking 8 mL 0.1 mol L^{-1} $KMnO_4$ without freeze-drying) and the $MnSO_4$ solution (32 mL 0.0625 mol L^{-1} $MnSO_4$) are mixed and heated in the sealed Teflon-lined autoclave for 12 h at 120 °C. Procedure C: The NGA (after soaking 8 mL 0.1 mol^{-1} $KMnO_4$ and freeze-drying) and the $MnSO_4$ solution (40 mL 0.05 mol L^{-1}) are mixed and heated in the sealed Teflon-lined autoclave for 12 h at 120 °C. As shown in **Fig. S1c**, the weight increase of the product from procedure C is the highest among these three samples, suggesting the most efficient loading of MnO_2. For the synthetic procedure A, the reaction between $KMnO_4$ and $MnSO_4$ starts from outside of NGA, and quite a few MnO_2 may form outside NGA. For procedure B, NGA without freeze-drying is fulfill with the $KMnO_4$ solution. These $KMnO_4$ will easily diffuse to the external surface of NGA, and some MnO_2 will still form outside NGA. For

procedure C, the $KMnO_4$ in NGA is in solid state after freeze-drying. In this case, most of the reactions between $KMnO_4$ and $MnSO_4$ happen inside the pores of NGA, and MnO_2 species form mainly inside NGA, leading to the highest MnO_2 content among these three synthetic procedures. If we compare the procedure B and C, during which the reactions between $MnSO_4$ and $KMnO_4$ mostly would happen inside NGA, the only difference is that whether there is solvent inside NGA. We think that with the freeze-drying process in procedure C, the $KMnO_4$ solid would be "confined" inside but not diffuse outside NGA, leading to larger amount of the reactions happen inside NGA. That is the reason why the product from procedure C has higher content of MnO_2 than from procedure B, and the freeze-drying process would indeed enhance the loading content of MnO_2.

SEM image and the electrochemical performance of the product without freeze-drying are shown in **Fig. S1d**. As shown in the SEM image, there is less MnO_2 formed inside the NGA in the product from procedure B than that from procedure C. The GCD cures of product from procedure B shows the specific capacity of 216.6 mAh g^{-1} at 0.1 A g^{-1}, which is lower than the specific capacity of MnO_2/NGA obtained from procedure C (275.8 mAh g^{-1} at 0.1 A g^{-1}).

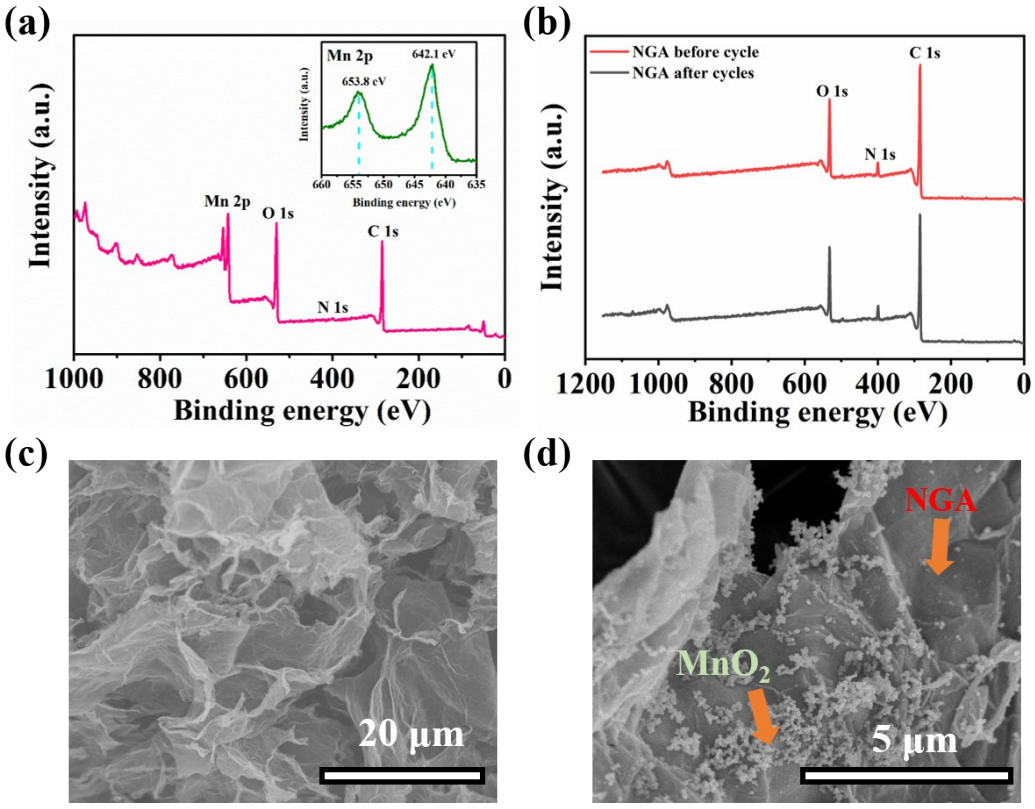

Fig. S2. (a) XPS spectra of the MnO_2/NGA (the inset illustrates the narrow spectra of Mn 2P peaks). (b) XPS spectra of the NGA before cycle and after cycles as electrode for Zn supercapacitor. (c) SEM image of NGA. (d) SEM image of MnO_2/NGA.

Table S1. C, O, N and Mn contents (atomic concentration %) in MnO_2/NGA from XPS.

Samples	C	O	N	Mn
MnO_2/NGA	60.72	26.41	1.42	11.45

Table S2. C, O, N, Zn and Mn contents (atomic concentration %) in NGA before and after charging/discharging cycles

Samples	C	O	N	Zn	Mn
NGA before cycle	81.52	15.24	3.18	0.06	0
NGA after cycles	80.32	15.97	3.43	0.12	0.16

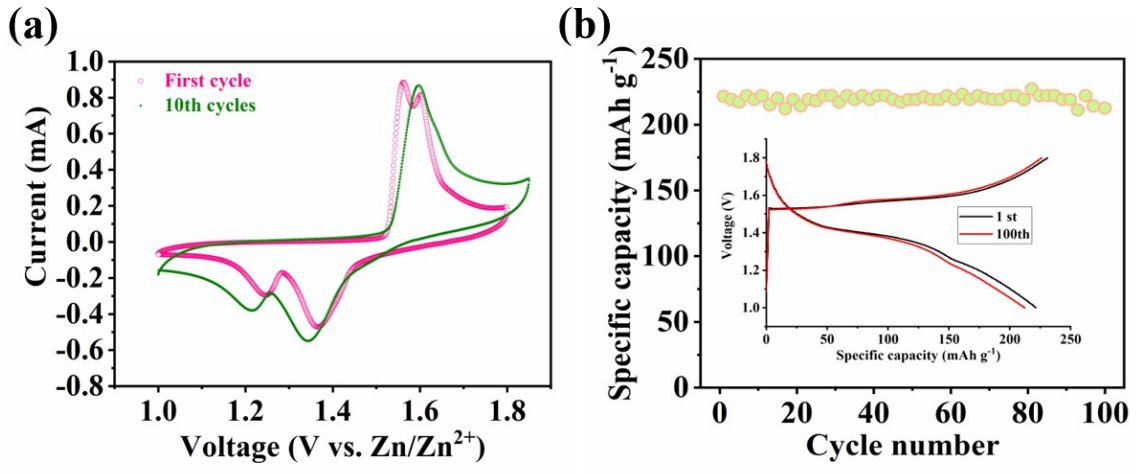

Fig. S3. (a) CV curves of the MnO_2/NGA at 0.1 mV s^{-1} (the first and the 10th cycle). (b) Cycling performance at the current density of 0.5 A g^{-1} with the inset as the GCD curves at the initial stage and after 100 cycles.

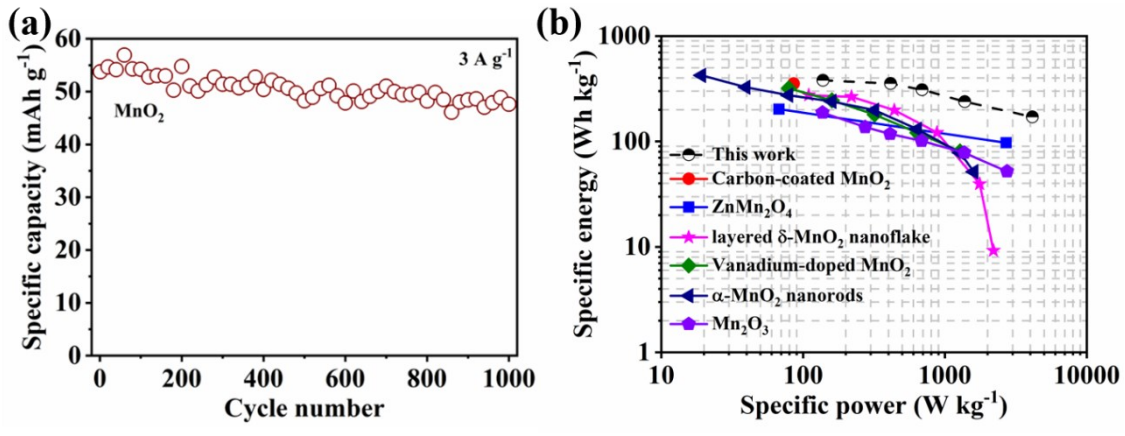

Fi

g. S4. (a) Long-term cycling performances of the MnO_2 at 3 A g^{-1}. (b) Comparison of the Ragone plot of the MnO_2/NGA-based battery with some other cathode materials for ZIB.

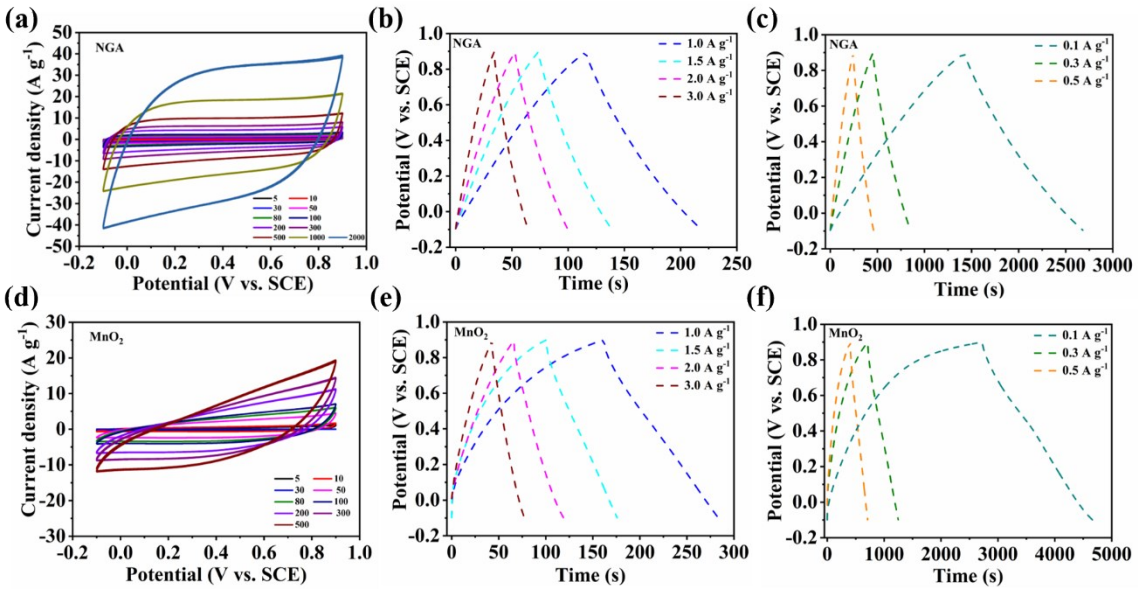

Fig. S5. (a) CV cures of the NGA at different scan rate from 5 mV s^{-1} to 2000 mV s^{-1}. (b, c) GCD cures of the NGA at different current densities from 0.1 A g^{-1} to 3 A g^{-1}. (d) CV curves of the MnO_2 at different scan rate from 5 mV s^{-1} to 500 mV s^{-1}. (e, f) GCD curves of the MnO_2 at different current densities from 0.1 A g^{-1} to 3 A g^{-1}.

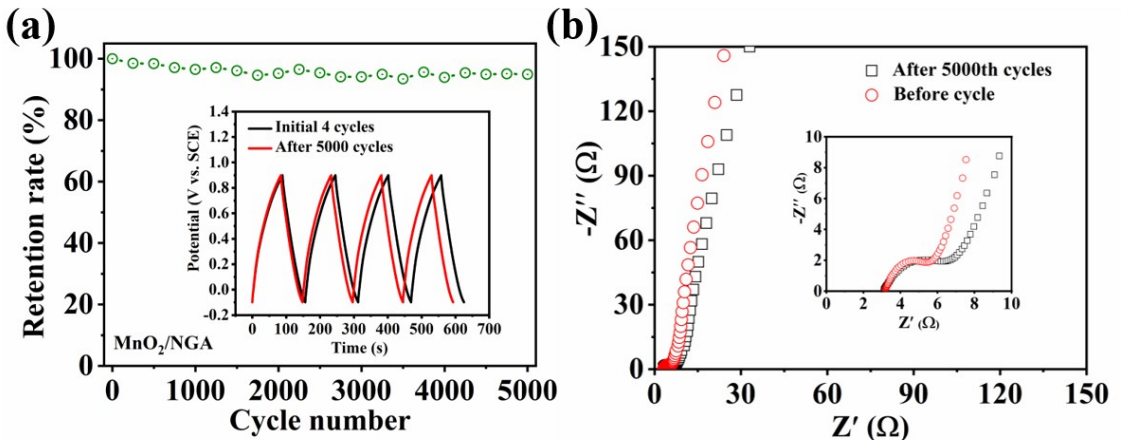

Fig. S6. (a) Cycling stability of the MnO_2/NGA at a current density of 3 A g^{-1} with the GCD curves after 5000 cycles as the inset. (b) Nyquist plots of experimental impedance date for the MnO_2/NGA in the frequency range of 100 kHz – 0.1 Hz before and after 5000 cycles with inset of the enlarged EIS.

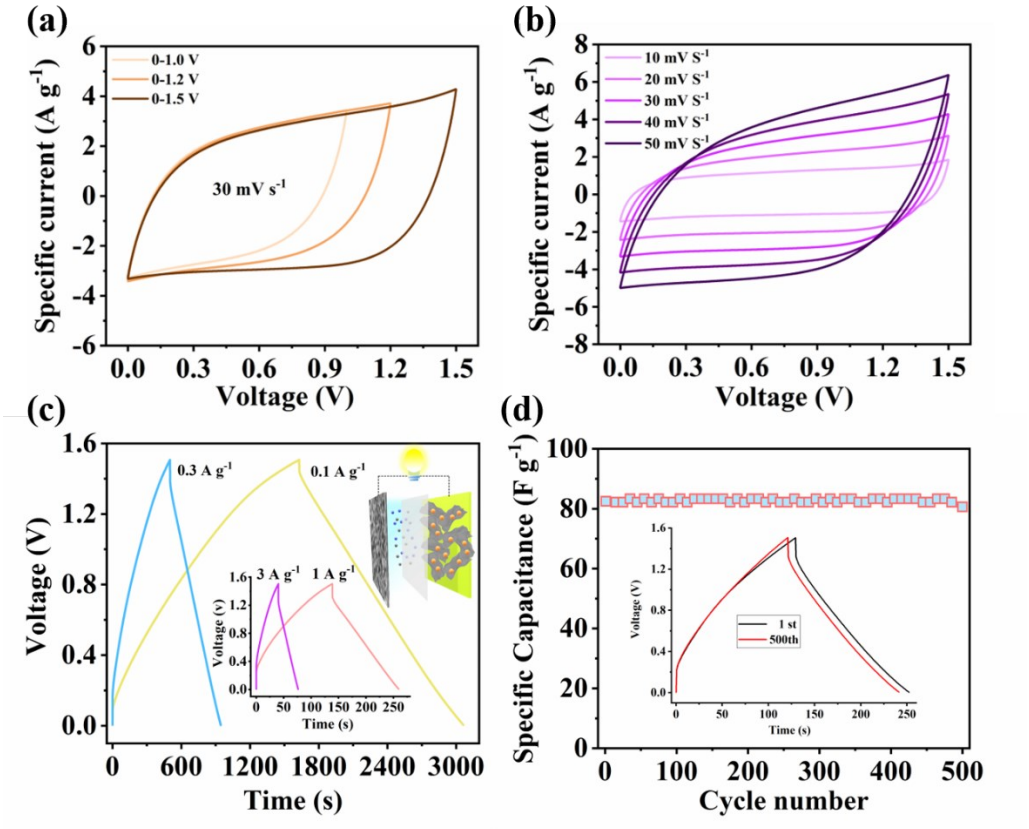

Fig. S7. Capacitive performance of the asymmetric supercapacitor (porous carbon//MnO_2/NGA). (a) CV curves with different voltage windows at a scan rate of 30 mV s^{-1}. (b) CV curves with a voltage window of 1.5 V at different scan rates. (c) GCD curves at different current densities. (d) Cycling performance at a current density of 1 A g^{-1} with the inset as the GCD curves at the initial stage and after 500 cycles.